Available online at www.sciencedirect.com
SCIENCE DIRECT®
Chemical Physics Letters 403 (2005) 185–191
CHEMICAL PHYSICS LETTERS
www.elsevier.com/locate/cplett

Nucleus–nucleus correlation function in non-Born–Oppenheimer molecular calculations: vibrationally excited states of HD^+

Sergiy Bubin *, Ludwik Adamowicz

Department of Chemistry, University of Arizona, Old Chemistry Building, Room 331, 1118 East Fourth Street, Box 210081, Tucson, AZ 85721-0081, USA
Department of Physics, University of Arizona, Tucson, AZ 85721, USA

Received 15 December 2004; in final form 4 January 2005
Available online 18 January 2005

Abstract

In the present work, we studied HD^+ (*dpe*) molecular ion in the framework of variational method without assuming the Born–Oppenheimer approximation. The non-adiabatic wave function was expanded in terms of explicitly correlated Gaussian basis functions. An algorithm for calculating the nucleus–nucleus correlation function (i.e., the probability density of one nucleus in the reference frame where the other one is at the origin) was derived, implemented, and used to depict all bound states of HD^+ with zero rotational energy.

1. Introduction

In recent years we have been involved in the development and implementation of methods that allow rigorous description of atomic and molecular systems without using the Born–Oppenheimer (BO) approximation regarding the separability of the electronic and nuclear motions. For an overview of this work, please see our recent reviews [1,2]. In the non-BO work performed in our laboratory we have used explicitly correlated multi-particle Gaussian basis functions (ECGs) for the wave function expansion. So far we have used three types of ECG basis sets. The simplest one employed in calculations of small atoms [3] consists of simple Gaussian exponentials dependent on the vector, $\mathbf{r}$, of the Cartesian coordinates describing the position of each particle (pseudo-particle) in an internal coordinate system,

$$\mathbf{r}_i = \begin{pmatrix} x_i \\ y_i \\ z_i \end{pmatrix}, \qquad \mathbf{r} = \begin{pmatrix} \mathbf{r}_1 \\ \mathbf{r}_2 \\ \cdots \\ \mathbf{r}_n \end{pmatrix} \tag{1}$$

and has the following form:

$$\phi_k = \exp[-\mathbf{r}'(A_k \otimes I_3)\mathbf{r}], \tag{2}$$

where A_k is a symmetric $n \times n$ matrix of variational exponential parameters, I_3 is the 3×3 identity matrix, $(')$ denotes transposition, and $\otimes$ is the Kronecker matrix product. The second basis involves even preexponential powers of the internuclear distance, $r_1^{m_k}$, and has been applied in calculations of ground and excited states of small diatomic systems [4–6]. The basis functions have the following form:

$$\varphi_k = r_1^{m_k} \exp[-\mathbf{r}'(A_k \otimes I_3)\mathbf{r}]. \tag{3}$$

The third basis consisting of ECGs with shifted centers (or floating spherical explicitly correlated Gaussians, FSECGs)

$$\omega_k = \exp\left[-(\mathbf{r} - \mathbf{s}_\mathbf{k})'(A_k \otimes I_3)(\mathbf{r} - \mathbf{s}_\mathbf{k})\right], \tag{4}$$

* Corresponding author. Fax: +1 520 621 8407.
E-mail address: bubin@email.arizona.edu (S. Bubin).

0009-2614/$ - see front matter © 2005 Elsevier B.V. All rights reserved.
doi:10.1016/j.cplett.2005.01.009

have been applied in non-BO calculations of static electrical properties of small diatomic systems [7–10] as well as in non-BO calculations on some small triatomic systems [11].

The internal Hamiltonian we use in non-BO calculations is obtained by explicit separation of the center-of-mass Hamiltonian from the complete Hamiltonian of the system expressed in the laboratory frame of coordinates. The origin of the internal coordinate system is placed at one of the nuclei (called the reference nucleus). Since the internal Hamiltonian is spatially isotropic (see Section 2), the bound non-adiabatic wave functions of an atomic or a molecular system form a fully symmetric representation of the rotational group. This implies that the internal ground-state wave function of any molecule is always spherically symmetric with respect to all rotations around the origin of the internal coordinate system. This is the property of the basis set (3) used in our approach in diatomic non-BO calculations including the HD^+ calculations described in our recent work [12]. In those calculations we determined all 23 rotationless states of HD^+ (in the conventional Born–Oppenheimer terminology those states are called vibrational states) and demonstrated that in the highest two states a significant charge asymmetry occurs leading to polarization of the system and formation of what can be described as a D–*p* complex. In essence, the bond in HD^+, which can be described as covalent in the first 21 states, becomes strongly ionic in the highest two states. This purely non-adiabatic effect is a result of near degeneracy of the *gerade* and *ungerade* electronic wave functions, and similar near degeneracy of closely located vibrational states near the dissociation threshold.

In the non-BO calculation of a molecular system, the wave function has to describe the coupled motion of the nuclei and electrons. The basis functions used to expand the wave function must correctly reflect this coupling. While the state of electrons can be very well represented with basis functions localized at atomic centers, the motion of the nuclei has to be described by functions that represent strongly reduced probability of two nuclei being found near each other (the Coulomb hole). Since the non-BO calculations have to be performed with very high accuracy (the non-adiabatic effects are very small), the success of such calculations strongly depends on the basis functions used. It has been shown in our previous calculations that, in the absence of the nucleus–nucleus interaction (i.e., for the atomic case), basis set (2) performs very well [3]. However, the application of this basis, even to small molecules (e.g. H_2^+, H_2), failed. This was due to the fact that simple correlated Gaussians centered at the origin of the coordinate system poorly describe a system where main portion of the density (i.e., nuclear density) is shifted away from the origin. Such a shift occurs for the nuclear density due to the repulsion interaction between the nuclei. To correct the problem, we introduced basis (3). The $r_1^{m_k}$ factor in this basis (where r_1 is the internuclear distance) shifts the maximum of the nuclear density away from the origin of the coordinate system where the reference nucleus is located. With m_k ranging from 0 to 250, this effect can be very effectively described as it has been demonstrated for several systems where our calculations produced more accurate results than had ever been obtained by others [7–10].

The main purpose of this work is to introduce the procedure for calculating nucleus–nucleus correlation function based on the non-BO diatomic wave function expanded in terms of basis functions (3). In the absence of a definite molecular structure, such as the one obtained in a BO calculation, the density plots provide complementary information to the expectation values of the structural parameters. For HD^+ such parameters were calculated in our previous work on this system [12]. They included the averaged distance between the deuteron and the proton, as well as the averaged distances between the deuteron and the electron, and the proton and the electron [12]. The latter two are the parameters that allowed us to conclude that in the two vibrational states the electron becomes almost entirely localized around the deuteron. In the present study we show how the nucleus–nucleus correlation function changes with the increase of the vibrational quantum number.

2. Hamiltonian, wave function, and pseudoparticle densities

The complete non-relativistic Hamiltonian for HD^+ in the laboratory Cartesian coordinate system is (in atomic units)

$$\hat{H}_{\mathrm{TOT}} = -\sum_{i=1}^{3} \frac{1}{2M_i} \nabla_{\mathbf{R}_i}^2 + \sum_{i=1}^{3} \sum_{j>i}^{3} \frac{Q_i Q_j}{R_{ij}}, \tag{5}$$

where M_i's, Q_i's, and $\mathbf{R}_i$'s are the masses, the charges, and the position vectors of the particles, respectively ($M_1 = m_d$, $M_1 = m_p$, $M_1 = m_e$, $Q_1 = 1$, $Q_2 = 1$, $Q_3 = -1$), and where $R_{ij} = |\mathbf{R}_j - \mathbf{R}_i|$ are interparticle distances. Note that no distinction between the electrons and the nuclei is made and the two types of particles are treated equivalently. In the next step, we transform the laboratory coordinate system to a new coordinate system [1,2], whose first three coordinates are the Cartesian coordinates describing the position of the center of mass in the laboratory coordinate frame and the remaining six coordinates are internal coordinates. The internal coordinates are defined with respect to a Cartesian coordinate system whose origin is placed at the deuteron and whose axes are parallel to the axes of the laboratory

coordinate frame. The first three of the six internal coordinates, defined as $\mathbf{r}_1 = \mathbf{R}_2 - \mathbf{R}_1$, describe the position of the proton with respect to the coordinate origin and the last three, $\mathbf{r}_2 = \mathbf{R}_3 - \mathbf{R}_1$, describe the position of the electron. Using the new coordinates, we can separate the Hamiltonian representing the motion of the center-of-mass in the laboratory coordinate system from the total Hamiltonian, $\hat{H}_{\mathrm{TOT}}$, thereby reducing the three-particle problem to a two-pseudoparticle problem. The internal Hamiltonian has the following form:

$$\hat{H} = -\frac{1}{2}\left(\sum_i^2 \frac{1}{m_i}\nabla^2_{\mathbf{r}_i} + \sum_{i\neq j}^2 \frac{1}{M_1}\nabla'_{\mathbf{r}_i}\nabla_{\mathbf{r}_j}\right) + \sum_{i=1}^2 \frac{q_0 q_i}{r_i} + \sum_{i<j}^2 \frac{q_i q_j}{r_{ij}}. \quad (6)$$

This Hamiltonian describes a system of two pseudoparticles, or internal particles, with masses $m_1 = m_{\mathrm{d}}m_{\mathrm{p}}/m_{\mathrm{d}} + m_{\mathrm{p}}$ and $m_2 = m_{\mathrm{d}}m_{\mathrm{e}}/m_{\mathrm{d}} + m_{\mathrm{e}}$, and charges $q_1 = 1$ and $q_2 = -1$ moving in the spherical potential generated by the $q_0 = 1$ charge of the reference particle located at the origin of the coordinate system. Thus, the wave function describing the internal state of the system, $\Psi(\mathbf{r}_1,\mathbf{r}_2)$ is dependent on the Cartesian coordinates of two pseudoparticles, the first resembling the proton ($\mathbf{r}_1$) and the second resembling the electron ($\mathbf{r}_2$). The second term in the parentheses in Eq. (6) is the mass polarization term, which arises from the coordinate transformation and which couples the motion of the two pseudoparticles. In the potential energy term, r_i and r_{ij} are defined as: $r_i = |\mathbf{R}_{i+1} - \mathbf{R}_1|$ and $r_{ij} = |\mathbf{R}_{j+1} - \mathbf{R}_{i+1}| = |\mathbf{r}_j - \mathbf{r}_i|$.

As we have noted in previous works, and as has been described by Monkhorst [13], this model of the molecule is quite similar to an atom. We have the analogue of the nucleus with the reference particle (deuteron) at the origin of the internal coordinate system, and we have the analogues of electrons in the pseudoparticles (see our previous work [11], or the work of Monkhorst [13], for further discussion). However, as it is in the case of HD^+, some of the pseudoparticles can be significantly heavier than the electrons and can have positive charges.

The HD^+ wave functions, $\Psi(\mathbf{r}) = \Psi(\mathbf{r}_1,\mathbf{r}_2)$, for all 23 rotationless states were generated in our previous work [12] using 2000-term expansions in a basis of ECG's with preexponential powers (3)

$$\Psi(\mathbf{r}) = \sum_{k=1}^{K} c_k \varphi_k(\mathbf{r}). \quad (7)$$

These wave functions were used here to calculate the one-pseudoparticle density associated with pseudoparticle 1 (i.e., pseudoproton) using the following formula:

$$g(\boldsymbol{\xi}) = \langle \Psi(\mathbf{r})|\delta(\mathbf{r}_1 - \boldsymbol{\xi})|\Psi(\mathbf{r})\rangle = \int_{-\infty}^{\infty} |\Psi(\boldsymbol{\xi},\mathbf{r}_2)|^2 \, \mathrm{d}\mathbf{r}_2, \quad (8)$$

where $\delta(\mathbf{r}_1 - \boldsymbol{\xi})$ is the 3D Dirac delta function. The pseudoparticle 1 density is equivalent to the correlation function of particles 1 and 2 (i.e., the deuteron and the proton). Thus, these two terms can be used interchangeably. The pseudoparticle density $g(\boldsymbol{\xi})$ calculation requires evaluation of the following matrix elements:

$$g_{kl}(\boldsymbol{\xi}) = \langle \varphi_k(\mathbf{r})|\delta(\mathbf{r}_1 - \boldsymbol{\xi})|\varphi_l(\mathbf{r})\rangle. \quad (9)$$

The algorithm for calculating these matrix elements is given in Appendix A.

We should note that the pseudoparticle density satisfies the following normalization condition:

$$\int_{-\infty}^{\infty} g(\boldsymbol{\xi}) \, \mathrm{d}\boldsymbol{\xi} = 4\pi \int_0^{\infty} g(\xi)\xi^2 \, \mathrm{d}\xi = 1. \quad (10)$$

3. Results

Since in the non-adiabatic calculations both electrons and nuclei are described on equal footing as quantum particles, the only available information about the molecular structure is contained in the electron–nucleus and nucleus–nucleus correlation functions. This is different from the conventional BO calculations where one can show molecular geometries in, for example, a ball and stick form, and electronic densities localized around the nuclei and at the bonds.

For all the considered states of HD^+, the wave functions are symmetric with respect to any rotation around the center of the internal coordinate system, but they differ in the number of radial nodes. The radial nodes should occur in terms of the $r_1 = |\mathbf{r}_1|$ coordinate because this coordinate represents the relative distance between the two nuclei in HD^+. Our calculations of the expectation values of the interparticle distances [12] showed that a strong charge asymmetry occurs in the system in the highest two vibrational states. Thus, it is interesting to see if those two states also differ from the other states in terms of the pseudoproton density.

In this work, we present 2D and 3D plots of the pseudoparticle 1 density. Since the wave functions are spherically symmetric, the 2D plots of the pseudoparticle 1 density, $g(\xi)$ ($\xi = |\boldsymbol{\xi}|$), should fully describe the behavior of this quantity. However, the 3D plot [i.e., the plot of $g(\xi_x,\xi_y,0)$] perhaps better represents the fully spherically symmetric nature of the pseudoparticle density function. In Fig. 1 we show the 2D pseudoproton density for the ground state and for the second, ninth, twentieth, twenty first, and twenty second excited states (i.e., the states with the vibrational quantum numbers, $v = 0$, 2, 9, 20, 21, and 22). The 3D plots of the pseudoproton density for the ground state and the second, third, and ninth excited states are shown in Fig. 2. As expected, the number of oscillations on these plots increases with the excitation level. Also, the spatial

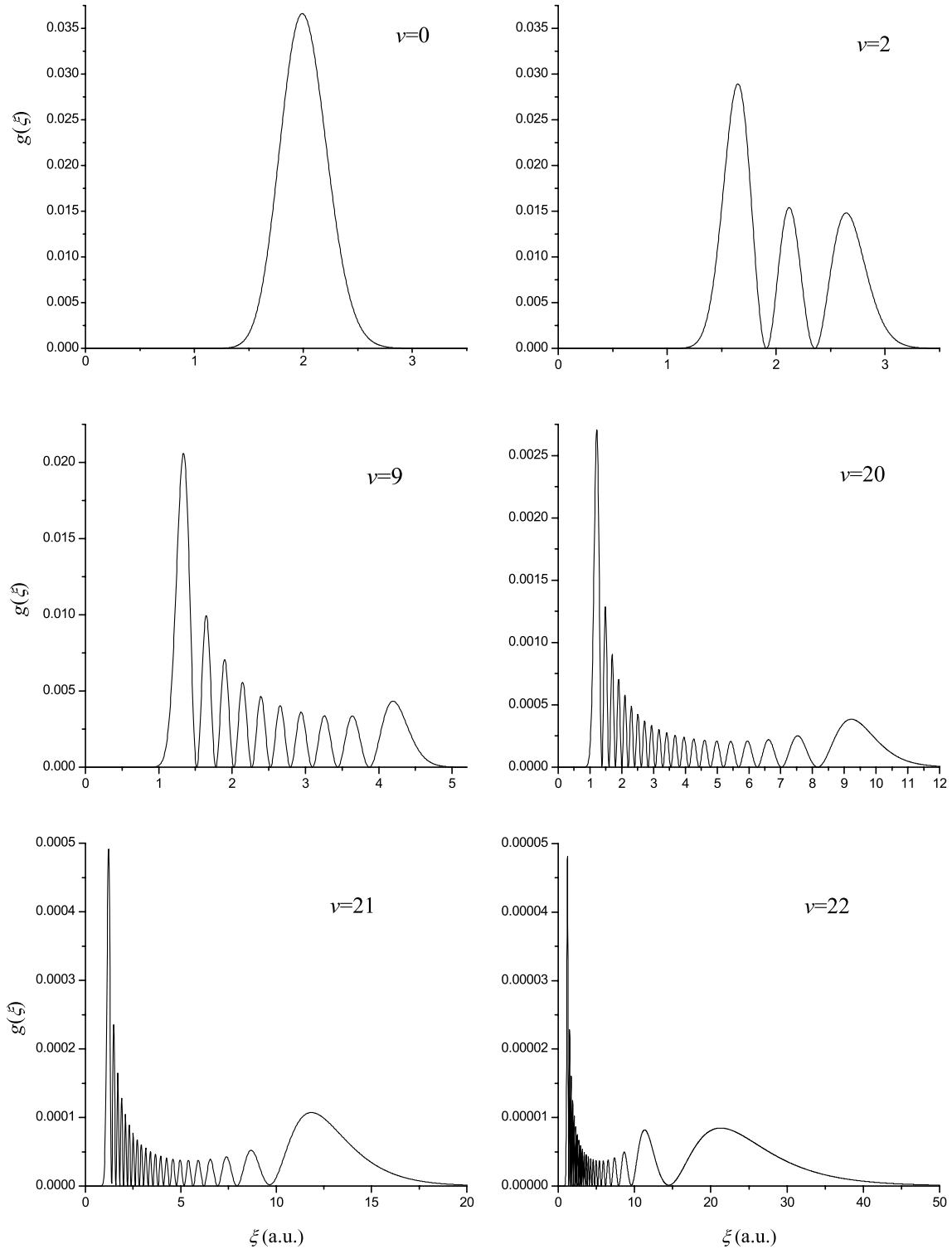

Fig. 1. 2D correlation function plots for the ground state, the second, ninth, twentieth, twenty first, and twenty second excited states of HD^+.

extent of the pseudoparticle density increases with the excitation. In higher excited states, though the density shows many oscillations, the highest density maximum is still the one closest to the origin of the coordinate system.

The states with $v = 21$ and 22 are the highest two excited states near the dissociation threshold. The spatial extent of the density dramatically increases for these states in comparison with the lower states. Also, in these highest two states ('the ionic states'), the last den-

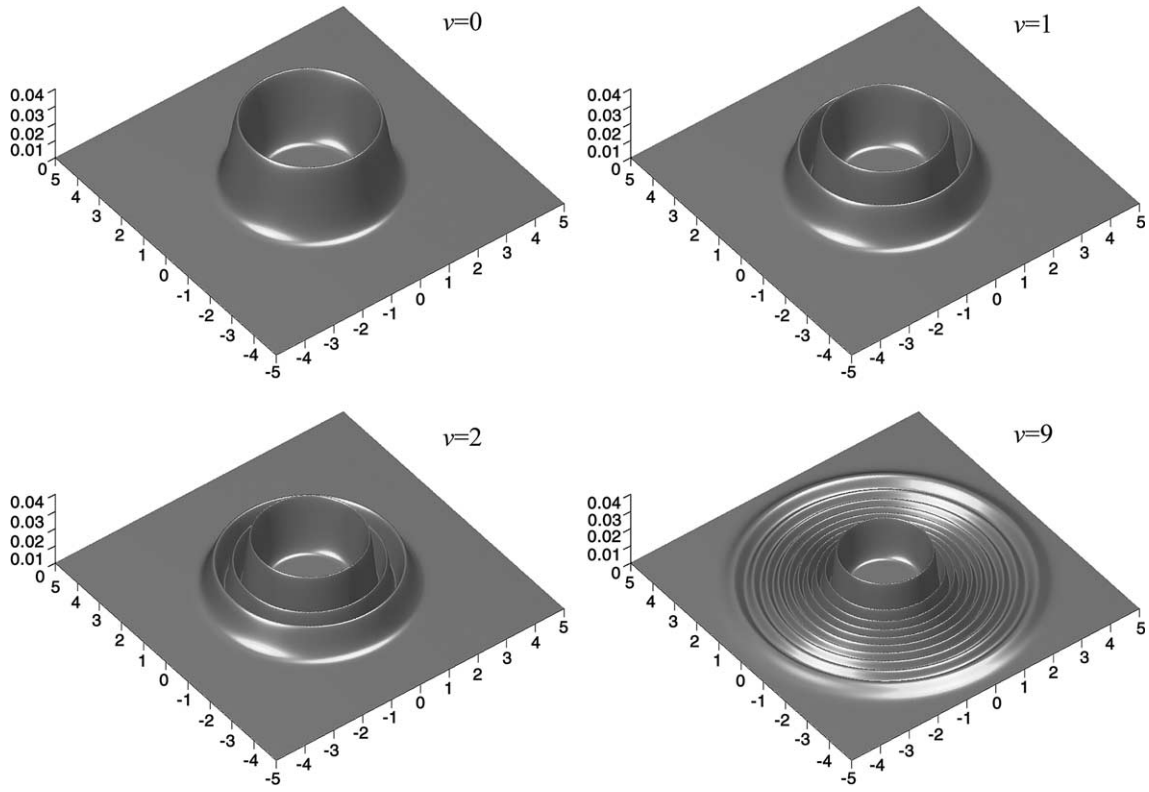

Fig. 2. 3D correlation function plots for the ground state, the second, third, and ninth excited states of HD^+ in the same scale. ξ_x and ξ_y (x- and y-axis, respectively) are in a.u.

sity maximum counting from the origin becomes much more prominent, indicating that in those states the two nuclei spend more time being significantly separated from each other than being close to each other. By comparing the pseudonucleus density of the highest 'covalent' state ($v = 20$) also shown in Fig. 1 with the densities of the 'ionic' $v = 21$ and 22 states one may notice a significant difference in the spatial diffuseness of the states and in the height of the last maximum. These differences are consistent with describing the HD^+ system in the latter two states as a complex of the D atom interacting with a proton. This seems to be a distinctive feature of the two states in comparison to the other (more 'covalent') states, where the electron is more evenly distributed between the two nuclei.

4. Conclusions

We have presented a study of the nucleus–nucleus correlation function (pseudoparticle 1 density) for the HD^+ molecular ion without using the Born–Oppenheimer approximation. In view of the lack of a definite molecular structure (such as the one resulting from a BO calculation), this correlation function provides a representation of the calculated state and a tool for its analysis. The correlation function plots for HD^+ show increasing oscillatory behavior with the increasing level of excitation. For the highest two excited vibrational states, where the bond becomes strongly ionic (as shown by the calculations of the averaged values of the interparticle distances [12]), the behavior of the correlation function shows some differences in comparison with lower states where the bond of the system is almost 100% covalent. The major difference is the increase of the correlation function at larger internuclear separations. This is consistent with the results for the average internuclear distance which also showed a significant increase for the higher two states. The nucleus–nucleus correlation function plots will provide particularly useful information for the analysis of non-BO wave functions in calculations of larger molecular systems excited both vibrationally and rotationally. Calculations of these types of states are the aim of our future studies.

Appendix A. Matrix elements for the non-BO nucleus–nucleus correlation function

To evaluate the matrix elements $g_{kl}(\boldsymbol{\xi}) = \langle \varphi_k(\mathbf{r}) | \delta(\mathbf{r}_1 - \boldsymbol{\xi}) | \varphi_l(\mathbf{r}) \rangle$ we will use some of the results from

previous works [14,15]. First, we need the value of the multi-dimensional Gaussian integral

$$\int_{-\infty}^{+\infty} \exp[-x'Ax + y'x]\,\mathrm{d}x = \frac{\pi^{n/2}}{|A|^{1/2}} \exp\left[\frac{1}{4}y'A^{-1}y\right]. \tag{A.1}$$

The integration here is over n variables, x is an n-component vector of these variables, y is a constant vector, $n\times n$ matrix A is assumed to be symmetric and positive definite. The expression for the overlap between simple spherical Gaussians (2) follows directly from (A.1). If we define $A_{kl} = A_k + A_l$, then

$$\langle\phi_k|\phi_l\rangle = \frac{\pi^{3n/2}}{|A_{kl}|^{3/2}}, \tag{A.2}$$

where the vertical bars denote the determinant of a matrix.

The matrix element of the Dirac delta function with two simple spherical Gaussians can be obtained using the Gaussian representation of the delta function

$$\delta(\mathbf{r}_1 - \boldsymbol{\xi}) = \lim_{\alpha\to\infty}\left(\frac{\alpha}{\pi}\right)^{3/2} \exp\left[-\alpha(\mathbf{r}_1 - \boldsymbol{\xi})^2\right]. \tag{A.3}$$

With this,

$$\langle\phi_k|\delta(\mathbf{r}_1 - \boldsymbol{\xi})|\phi_l\rangle = \lim_{\alpha\to\infty}\frac{\alpha^{3/2}}{\pi^{3/2}}\langle\phi_k|\exp\left[-\alpha r_1^2 + 2\alpha\mathbf{r}_1\boldsymbol{\xi} - \alpha\xi^2\right]|\phi_l\rangle. \tag{A.4}$$

The square of r_1 can be conveniently represented using J_{11} matrix of rank 1 whose all elements are zeros except element 11, which is equal to 1

$$r_1^2 = \mathbf{r}'(J_{11}\otimes I_3)\mathbf{r}. \tag{A.5}$$

Then,

$$\begin{aligned}\langle\phi_k|\delta(\mathbf{r}_1 - \boldsymbol{\xi})|\phi_l\rangle &= \lim_{\alpha\to\infty}\frac{\alpha^{3/2}}{\pi^{3/2}}\langle\phi_k|\exp\left[-\alpha\mathbf{r}'(J_{11}\otimes I_3)\mathbf{r} + 2\alpha(j_1\otimes\boldsymbol{\xi})'\mathbf{r} - \alpha\xi^2\right]|\phi_l\rangle \\ &= \lim_{\alpha\to\infty}\frac{\alpha^{3/2}}{\pi^{3/2}}\frac{\pi^{3n/2}}{|A_{kl} + \alpha J_{11}|^{3/2}} \times \exp\left[\alpha(j_1\otimes\boldsymbol{\xi})'[(A_{kl} + \alpha J_{11})\otimes I_3]^{-1}(j_1\otimes\boldsymbol{\xi}) - \alpha\xi^2\right]\end{aligned} \tag{A.6}$$

In the last expression we used the relation (A.1). j_1 is an n-component vector whose first element is equal to 1 and the rest are zeros.

Since J_{11} is a rank 1 matrix, we can write the determinant in the last formula as

$$\begin{aligned}|A_{kl} + \alpha J_{11}| &= |A_{kl}||I_n + \alpha A_{kl}^{-1}J_{11}| \\ &= |A_{kl}|(1 + \alpha\mathrm{tr}[A_{kl}^{-1}J_{11}]),\end{aligned} \tag{A.7}$$

where tr [...] denotes the trace of a matrix and I_n is an $n\times n$ identity matrix. As the limit of the preexponential part of (A.6) is a finite number, the limit of the exponent must be equal to $-\beta\xi^2$, with β being a finite number. Otherwise the entire expression (A.6) would have been either zero or infinity, which is not the case. Hence,

$$\begin{aligned}\langle\phi_k|\delta(\mathbf{r}_1 - \boldsymbol{\xi})|\phi_l\rangle &= \frac{\pi^{3(n-1)/2}}{|A_{kl}|^{3/2}}\frac{1}{\mathrm{tr}[A_{kl}^{-1}J_{11}]^{3/2}}\exp[-\beta\xi^2] \\ &= \langle\phi_k|\phi_l\rangle\frac{1}{\pi^{3/2}}\frac{1}{\mathrm{tr}[A_{kl}^{-1}J_{11}]^{3/2}}\exp[-\beta\xi^2].\end{aligned} \tag{A.8}$$

Making use of the normalization condition,

$$\int_{-\infty}^{\infty}\langle\phi_k|\delta(\mathbf{r}_1 - \boldsymbol{\xi})|\phi_l\rangle\,\mathrm{d}\boldsymbol{\xi} = \langle\phi_k|\phi_l\rangle, \tag{A.9}$$

we can easily find that $\beta = \mathrm{tr}[A_{kl}^{-1}J_{11}]^{-1}$. Thus,

$$\langle\phi_k|\delta(\mathbf{r}_1 - \boldsymbol{\xi})|\phi_l\rangle = \langle\phi_k|\phi_l\rangle\frac{1}{\pi^{3/2}}\frac{1}{\mathrm{tr}[A_{kl}^{-1}J_{11}]^{3/2}} \times \exp\left[-\frac{\xi^2}{\mathrm{tr}[A_{kl}^{-1}J_{11}]}\right]. \tag{A.10}$$

The last relationship is now used to evaluate the matrix elements of $\delta(\mathbf{r}_1 - \boldsymbol{\xi})$ with basis functions (3). To do that we differentiate (A.10) $p = (m_k + m_l)/2$ times with respect to a parameter, λ, and set the parameter to zero at the end. The procedure looks as follows:

$$\begin{aligned}\langle\varphi_k|\delta(\mathbf{r}_1 - \boldsymbol{\xi})|\varphi_l\rangle &= \langle\phi_k|r_1^{2p}\delta(\mathbf{r}_1 - \boldsymbol{\xi})|\phi_l\rangle \\ &= (-1)^p\frac{\partial^p}{\partial\lambda^p}\langle\phi_k|\exp\left[-\lambda\mathbf{r}'(J_{11}\otimes I_3)\mathbf{r}\right] \times \delta(\mathbf{r}_1 - \boldsymbol{\xi})|\phi_l\rangle|_{\lambda=0} \\ &= (-1)^p\frac{\partial^p}{\partial\lambda^p}\frac{\pi^{3n/2}}{|A_{kl} + \lambda J_{11}|^{3/2}}\frac{1}{\pi^{3/2}} \times \frac{1}{\mathrm{tr}[(A_{kl} + \lambda J_{11})^{-1}J_{11}]^{3/2}} \times \exp\left[-\frac{\xi^2}{\mathrm{tr}[(A_{kl} + \lambda J_{11})^{-1}J_{11}]}\right]\Bigg|_{\lambda=0}.\end{aligned} \tag{A.11}$$

Applying the following formulae:

$$\frac{\partial}{\partial\lambda}|A_{kl} + \lambda J_{11}| = |A_{kl} + \lambda J_{11}|\mathrm{tr}[(A_{kl} + \lambda J_{11})^{-1}J_{11}], \tag{A.12}$$

$$\frac{\partial}{\partial\lambda}\mathrm{tr}[(A_{kl} + \lambda J_{11})^{-1}J_{11}] = -\mathrm{tr}[(A_{kl} + \lambda J_{11})^{-1}J_{11} \times (A_{kl} + \lambda J_{11})^{-1}J_{11}] \tag{A.13}$$

and using the fact that $\mathrm{tr}\,[XJ_{11}XJ_{11}] = \mathrm{tr}\,[XJ_{11}]^2 = (X_{11})^2$ for an arbitrary matrix X reduces the final result to

$$\begin{aligned} g_{kl}(\boldsymbol{\xi}) &= \langle\varphi_k|\delta(\mathbf{r}_1-\boldsymbol{\xi})|\varphi_l\rangle \\ &= \langle\varphi_k|\varphi_l\rangle \frac{1}{2\pi}\frac{1}{\Gamma\left(p+\frac{3}{2}\right)} \\ &\quad\times \frac{1}{(A^{-1}_{kl})^{3/2}_{11}}\left[\frac{\xi^2}{(A^{-1}_{kl})_{11}}\right]^p \exp\left[-\frac{\xi^2}{(A^{-1}_{kl})_{11}}\right], \end{aligned} \tag{A.14}$$

where $\langle\varphi_k|\varphi_l\rangle$ is the overlap matrix element [15]

$$\begin{aligned} \langle\varphi_k|\varphi_l\rangle &= \left\langle\phi_k\middle|r_1^{2p}\middle|\phi_l\right\rangle \\ &= \frac{2}{\sqrt{\pi}}\Gamma\left(p+\frac{3}{2}\right)\mathrm{tr}\,[A^{-1}_{kl}J_{11}]^p\langle\phi_k|\phi_l\rangle \\ &= \frac{2}{\sqrt{\pi}}\Gamma\left(p+\frac{3}{2}\right)(A^{-1}_{kl})^p_{11}\langle\phi_k|\phi_l\rangle, \end{aligned} \tag{A.15}$$

and $\Gamma(x)$ is the Euler gamma function.

References

[1] M. Cafiero, S. Bubin, L. Adamowicz, Phys. Chem. Chem. Phys. 5 (2003) 1491.
[2] S. Bubin, M. Cafiero, L. Adamowicz, Adv. Chem. Phys. (submitted).
[3] D.B. Kinghorn, L. Adamowicz, J. Chem. Phys. 106 (1997) 4589.
[4] D.B. Kinghorn, L. Adamowicz, Phys. Rev. Lett. 83 (1999) 2541.
[5] C.E. Scheu, D.B. Kinghorn, L. Adamowicz, J. Phys. Chem. 114 (2001) 3393.
[6] S. Bubin, L. Adamowicz, J. Chem. Phys. 118 (2003) 3079.
[7] M. Cafiero, L. Adamowicz, Phys. Rev. Lett. 88 (2002) 33002.
[8] M. Cafiero, L. Adamowicz, J. Chem. Phys 116 (2002) 5557.
[9] M. Cafiero, L. Adamowicz, Phys. Rev. Lett. 89 (2002) 073001.
[10] M. Cafiero, L. Adamowicz, M. Duran, J.M. Luis, J. Mol. Struct. (THEOCHEM) 633 (2003) 113.
[11] M. Cafiero, L. Adamowicz, Chem. Phys. Lett. 387 (2004) 136.
[12] S. Bubin, E. Bednarz, L. Adamowicz, J. Chem. Phys. (in press).
[13] H.J. Monkhorst, Int. J. Quantum Chem. 72 (1999) 281.
[14] D.B. Kinghorn, Int. J. Quantum Chem. 57 (1996) 141.
[15] D.B. Kinghorn, L. Adamowicz, J. Chem. Phys. 110 (1999) 7166.